Bioelectrochemistry 135 (2020) 107549

Contents lists available at ScienceDirect

Bioelectrochemistry

journal homepage: www.elsevier.com/locate/bioelechem

Electricity from methanol using indigenous methylotrophs from hydraulic fracturing flowback water

Kalimuthu Jawaharraj [a,b], Namita Shrestha [c], Govind Chilkoor [a], Bhuvan Vemuri [a], Venkataramana Gadhamshetty [a,b,d,*]

[a] Civil and Environmental Engineering, South Dakota School of Mines and Technology, 501 E. St. Joseph Street, Rapid City, SD 57701, USA
[b] BuG ReMeDEE Consortia, South Dakota School of Mines and Technology, 501 E. St. Joseph Street, Rapid City, SD 57701, USA
[c] Civil and Environmental Engineering, University of Wisconsin-Platteville, 139 Ottensman Hall, 1 University Plaza Platteville, WI 53818, USA
[d] 2D-materials for Biofilm Engineering, Science and Technology (2DBEST) Center, South Dakota School of Mines and Technology, 501 E. St. Joseph Street, Rapid City, SD 57701, USA

ARTICLE INFO

Article history:
Received 21 November 2019
Received in revised form 2 May 2020
Accepted 5 May 2020
Available online 11 May 2020

Keywords:
Flowback water
Methylotrophs
Biofilms
Rhodobacter sphaeroides
Illumina sequencing
Microbial electrochemical system

ABSTRACT

Methanol solvents that are used in hydraulic fracturing often return back to the surface in the form of recalcitrant flowback water. Here, the indigenous methylotrophic bacteria from flowback water were enriched and used to generate electricity from methanol in a two-compartment microbial fuel cell (CH_3OH-MFC). An identical MFC based on a tryptone-yeast extract (TY-MFC) was used as a control. CH_3OH-MFC yielded a 2.7-fold thicker biofilm dominated by electrogenic species (81%) and higher power density (76 mW/m^2) compared with TY-MFC (50 mW/m^2). Illumina MiSeq sequencing of the 16S rRNA gene in TY-MFC revealed classes from *Actinobacteria, Bacteroidia* and *γ-proteobacteria*. The CH_3OH-MFC yielded *α-proteobacteria*, *β-proteobacteria*, *γ-proteobacteria* and *Bacteroidia*, with a dominant fraction of *Rhodobacter sphaeroides* (~29%). We discuss the potential pathways used by *R. sphaeroides* to maintain syntrophic cooperation with other bacterial and archaeal members to sustain CH_3OH oxidation. Finally, we establish that a pure culture of *R. sphaeroides* 2.4.1 generates electricity directly from methanol.

1. Introduction

Hydraulic fracturing and horizontal drilling methods are used to extract crude oil from previously inaccessible Bakken shale formation [1]. They convert a significant portion of injected fluid into recalcitrant wastewater ("*flowback water*"), a mixture of formation water and fracturing fluids. Due to the lack of viable treatment technologies, ~90% of the flowback water is transported and permanently disposed of into class II injection wells [2]. During transport, pipeline leakages and truck accidents have resulted in flowback water spills, threatening nearby water resources and agricultural lands [3]. Our earlier study provided a comprehensive review of potential water resource impacts due to both deterministic (flow water management) and probabilistic events (flowback pipeline spills and truck accidents) [2,4]. Hence, there is a need to develop robust microorganisms for enabling flowback water treatment and reuse technologies.

Prior studies have reported the adaptability, growth and biodiversity aspects of microorganisms in the wellhead [5,6], fracturing fluids and flowback water from fractured shales [7]. The chemical composition of the fracturing fluids influences the biodiversity of the indigenous microbial communities [8]. However, such reports on the microbial ecology in Bakken shale are yet sparse [5,6]. There is also a need to enrich and isolate beneficial microorganisms to treat the dominant hydrocarbons selectively in the flowback water. Methanol solvents are often used in the fracturing fluids to minimize corrosion, freezing, and friction during hydraulic fracturing [9]. Thus, flowback water contains methanol along with methane, formaldehyde, phenol and toluene [10,11], all of which promote the growth of "methylotrophs", microorganisms which can oxidize both methanol and methane substrates. One can expect drilling mud, geological formation, fluid amendments, handling water infrastructure, and flowback water to harbor methylotrophs [12]. The presence of methylotrophs in flowback water was recently established using a ^{13}C isotope labeling methods [11]. Such methylotrophs have been rarely observed in the samples extracted from natural environments [13]. Methylotrophs found in the flowback water have been found to display denitrifying anaerobic methane oxidation (DAMO) pathways and a unique ability to remediate

* Corresponding author at: Civil and Environmental Engineering, South Dakota School of Mines and Technology, 501 E. St. Joseph Street, Rapid City, SD 57701, USA.
E-mail address: Venkata.Gadhamshetty@sdsmt.edu (V. Gadhamshetty).

https://doi.org/10.1016/j.bioelechem.2020.107549
1567-5394/

heavy metals [14–16]. The current study aims to isolate and enrich methylotrophs for treating methanol in MFCs and microbial capacitive deionization units. Such processes can alleviate the disadvantages of energy-intensive desalination technologies including reverse osmosis [17].

Exoelectrogens are microorganisms that use the extracellular electron transfer processes to generate electricity from organic matter [18–20]. The current study builds upon our earlier work where we reported the use of exoelectrogens for reducing chemical oxygen demand (COD) in the flowback water [21]. This flowback water contains a high level of COD (1000 mg/L) [4] in the form of methanol, methane, and other hydrocarbons which may favor the growth of exoelectrogenic methylotrophs. The high levels of total dissolved solids (2.2 g/L) render flowback water as a suitable electrolyte in MFCs [21].

This study enriched the indigenous microbial consortia from Bakken shale in an MFC which was solely fed with methanol (CH_3-OH-MFC). Illumina MiSeq sequencing of the 16S rRNA gene confirmed that the CH_3OH-MFC yielded methylotrophs from the classes of α-proteobacteria, β-proteobacteria, γ-proteobacteria and Bacteroidia taxa, with a dominant fraction of *R. sphaeroides* (~29%). The microscopy studies corroborated the morphology and viability aspects of the methylotrophic biofilms in the CH_3OH-MFC. This study explored the syntrophic pathways used by the consortia to generate electricity from methanol. Finally, a proof of concept for electricity generation from methanol by *Rhodobacter sphaeroides* 2.4.1 was provided.

2. Materials and methods

2.1. MFC configuration

Both the CH_3OH-MFC and TY-MFC were based on the two-compartment MFC design used in our earlier study [21]. The volumetric capacity of the anode and cathode compartments was 180 mL each. The inter-electrode spacing was 0.005 m. Pretreated graphite felt discs (Φ = 0.064 m) were used as the anode and cathode, respectively. An Ultrex membrane was used to separate the two compartments. All the MFCs used a 50 mM ferricyanide as the catholyte. The consortia were enriched under closed-circuit conditions (R_{ext} = 100 Ω) using a three-step sequential process that lasted for nearly 270 days.

Phase-1: Conditioning in a saline media: The anode of a parent MFC was inoculated with flowback water samples from a fractured site at Bakken shale. The values of pH, COD, type and levels of anions and cations and other composition details of flowback water were described in our earlier study [2]. Noting that the consortia were originally exposed to high levels of total dissolved solids in the flowback water (~350 g/L), the consortia was initially enriched in conditions using the saline media (2.04 mM NaCl) [22]. The test MFCs were evaluated for soluble chemical oxygen demand ($sCOD_i$ = 1400 mg COD/L) in the form of methanol. Initial and final CODs were measured using Method 5220 Hach COD system and their COD removal efficiencies were calculated. This phase lasted for 1440 h under closed-circuit conditions (R_{ext} = 100 Ω).

Phase-2: Enrichment in rich media: 10% of the anolyte was used as inocula for the subsequent MFC tests throughout the study. Briefly, 20 mL of the anolyte from phase-1 was centrifuged at 8000 rpm for 20 min. The cell pellet was then resuspended aseptically in phosphate buffer and centrifuged to remove the residual NaCl. These saline free cells were used as inoculum in phase-2 MFC experiments. Two identical two-compartment MFCs operated in a fed-batch mode were used to enrich the consortia in a TY medium buffered with 50 mM phosphate for 90 days. After observing a steady-state electrical performance under the closed-circuit conditions, these brood MFCs were transitioned to the test phase.

Phase-3: CH_3OH-fed MFCs: The MFC experiments were run in a fed-batch mode. The brood MFCs were transitioned into a testing phase to evaluate the ability of the consortia to generate electricity from methanol in CH_3OH-MFCs. Briefly, the spent anolyte from the brood MFCs were drained completely, gently washed with the phosphate buffer, and refilled with the equivalent volume of methanol-supplemented nitrate mineral salt media. This test is designed to enrich electroactive methylotrophs using methanol as the electron donor and as the terminal electron acceptor. The enriched consortia were assessed for its ability to generate electric power from methanol. An identical brood MFC used TY as the anolyte was used *(herein referred to TY-MFC)*. An additional brood MFC was set up using 50 mM phosphate buffer media that lacked carbon substrate as the anolyte. The electrochemical performance of the enriched consortia was monitored using polarization tests and electrochemical impedance spectroscopy analysis. All of the MFCs were carried out under ambient light conditions (300 lx) available in a typical laboratory setting.

2.2. Electrochemical and gas chromatography measurements

2.2.1. Power density curves

Voltage data was acquired using a DAQ/54 module (I/O Tech Inc., Cleveland OH) across an external load (RS-200, IET Labs Inc., Westbury, NY). The polarization data at each resistance was recorded after 60 min to obtain the voltage values at steady-state conditions. Ohm's law was used to determine current and subsequently, power density using the voltage values from the polarization tests and corresponding values of external resistance (1 to 10,000 O).

2.2.2. Electrochemical impedance spectroscopy (EIS)

EIS measurements were carried out using a Gamry reference 3000 potentiostat with an amplitude of 10 mV. The frequency range was1000 kHz to 10 MHz and the DC bias was 60 mV. EIS data were fitted to a two-RC circuit consisting of solution resistance (R_{ohm}), constant phase element in biofilm (CPE_{film}), electrode double layer (CPE_{dl}), charge transfer resistance in biofilm (R_{film}) and electrode polarization resistance (R_p) along with Warburg impedance (Fig. 2b).

2.2.3. Cyclic voltammetry

Cyclic Voltammograms (CV) were obtained for the abiotic MFC, CH_3OH-MFC and TY-MFC on day 25 in the potentials of − 1.0 to 1.0 V vs. Ag/AgCl reference electrode at a scanning rate of 10 mV/s. The CV procedures were described in our earlier study [21,81]. The anode was used as the working electrode and cathode as the counter electrode. All the tests were carried out after ensuring adequate levels of the carbon substrates.

2.2.4. Gas chromatography analysis

To investigate the occurrence of methanogenesis in the CH_3OH-MFC and TY-MFC, we carried out a gas chromatography analysis (SRI Instruments, model 8610C, CA, USA) equipped with a thermal conductivity detector and a molecular sieve column (Restek Molesieve 5A 80/100 1.83 m × 38 mm × 26 mm). Injector, detector and column temperatures were kept at 100, 70 and 100 °C, respectively with argon as the carrier gas. The methane gas composition was identified based on the retention times of the standard methane. The injection volume was 1 mL.

2.3. Biofilm morphology, viability and thickness

The morphology of biofilms grown on the electrode surfaces was analyzed using a scanning electron microscopy (SEM). The electrodes were fixed using 3% glutaraldehyde in a sodium cacodylate buffer (0. 1 M, pH 7.2) for 2 h at room temperature (a modified procedure [23]. The fixed samples were gently rinsed with a sodium cacodylate buffer for three times and finally washed with double distilled water. The biofilm was sequentially dehydrated using a 50% and 100% acetone and dried overnight in a desiccator. Dried electrodes were visualized using a scanning electron microscope (Zeiss Supra40). Other sets of electrode samples were subjected to live/dead staining using the Filmtracer™ LIVE/DEAD™ Biofilm Viability Kit (Invitrogen, USA). The biofilm samples were also analyzed using an inverted fluorescent microscope (IX71, Olympus). The height profiles of biofilm samples were assessed using a 3D laser scanning microscopy (3D-LSM, Model solution-treated C2 Plus, Nikon, Tokyo, Japan).

2.4. Microbial community analysis

To analyze the microbial community at the end of phase-2 and phase-3, the enriched anolyte samples were centrifuged at 8000 rpm for 20 min at 4 °C. Total genomic DNA was extracted from the bacterial cell pellet using PureLink™ Microbiome DNA Purification Kit (ThermoFisher Scientific). An Illumina 2-step Miseq sequencing-based microbial diversity analysis was performed at the Research and Testing Laboratory (Lubbock, TX). The consortia from both the CH_3OH-MFC and TY-MFC were analyzed using an illumina 2-step Miseq sequencing procedure. The samples were amplified using a two-step process. The first step involved a PCR amplification using the illumina i5 sequencing forward primer and the illumina i7 sequencing reverse primer. Briefly, 25 μL reaction was performed using Qiagen HotStarTaq master mix (Qiagen Inc, Valencia, California) with 1 μL of forward and reverse primers (5 μM each) and 1 μL of template DNA. Reactions were performed on ABI Veriti thermocyclers (Applied Biosystems, Carlsbad, California) using the following thermal profile: 95 °C for 5 min, 35 cycles at 94 °C for 30 s, 54 °C for 40 s, 72 °C for 1 min, followed by a cycle of 72 °C for 10 min and finally held at 4 °C.

The PCR products from the first stage were further processed using the following Illumina Nextera PCR primers: forward primer (i5 index) and reverse primer (i7 index). The steps were similar to that in the first stage except that we used 10 cycles. Amplified PCR products were visualized with eGels (Life Technologies, Grand Island, New York). The PCR products were pooled in an equimolar fashion and each pool was size selected in two rounds using SPRIselect Reagent (Beckman Coulter, Indianapolis, Indiana) and in a 0.75 ratio for both the rounds. The size selected pools were quantified using the Qubit 4 Fluorometer (Life Technologies) and loaded on an Illumina Miseq (Illumina, Inc. San Diego, California) 2 × 300 flow cell at 10 pM. The microorganisms were identified based on the sequencing results which were compared against the available sequences in the database.

2.5. Photosynthetic MFCs using R. sphaeroides 2.4.1. pure cultures

To elucidate the electrogenic activity of *R. sphaeroides,* pure cultures of *R. sphaeroides* 2.4.1 were inoculated in an H-type batch MFCs containing fresh NMS media and methanol as the electron donor, graphite felt (surface area of 10 cm^2) as the anode and carbon brush (surface area of 130 cm^2) as cathode. 100 mM potassium ferricyanide in phosphate buffer (50 mM, pH 7.0) was used as catholyte. The pMFCs were operated under an external load of 150 Ω. To induce the photoheterotrophic mode of growth, the photosynthetic MFC (pMFC) system was illuminated by a light source at 700 lx intensity and the temperatures were maintained at 27 ± 2 °C. The distance between the lamp and the anode unit was 25 cm. Noting the liquid depth of 5 cm in the anode compartment, the actual distance between the lamp and the anode surface is 30 cm. The experiment was conducted for 30 days and the polarization curves and EIS were recorded every 5 days. To ascertain the exoelectrogenic capabilities of *R. sphaeroides,* we ran three additional MFC tests, including NMS media with methanol and inoculum (CH_3OH^+ RSP^+-MFC), NMS media with methanol and without inoculum (CH_3OH^+ RSP^--MFC) and NMS media without methanol and inoculum (CH_3OH^- RSP^--MFC). Coulombic efficiencies were calculated using Equation (1) shown below [24].

$$CE = \frac{\sum_{i=1}^{n} U_i t_i}{RFb\Delta SV} M \times 100\% \quad (1)$$

where U_i is the output voltage of MFC at time t_i, R is the external resistance, F is Faraday's constant (96,485 C/mol e), b is the number of moles of electrons produced per mol of COD (4 mol of e/ mol of COD), ΔS is the removal of COD concentration (g/L), V is the liquid volume (L), and M is the molecular weight of oxygen (32 g/mol).

3. Results and discussion

3.1. Electrochemical analysis

The average values of the OCV and current density during the conditioning phase were 0.5 V and 418.8 mA/m^2, respectively. During phase 3, the consortia did not generate any electricity in MFCs that lacked carbon substrate (not discussed further). A goal of this study was to establish the methylotrophic capabilities of the enriched consortia in MFCs. We assessed the electrical performance of the CH_3OH-MFC using the temporal profiles of OCV and power density (Figure S1). The temporal profiles of the current density during the conditioning phase confirmed the steady-state performance of the MFC (Figure S3). CH_3OH-MFC yielded superior compared with TY-MFC (fed with TY medium) (Fig. 1, Figure S1). While the OCV values in both CH_3OH-MFC and TY-MFC were similar (~0.7 V), the peak power density in CH_3OH-MFC (76 mW/m^2)

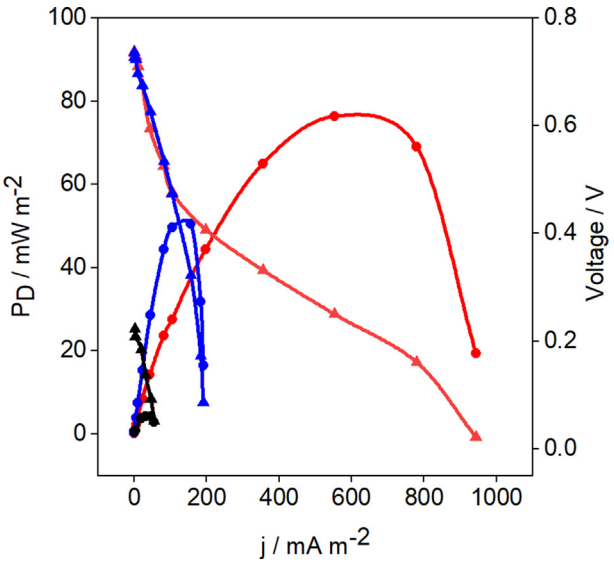

Fig. 1. Bioelectrochemcial performances of MFCs. Comparison of power density yields from the CH_3OH-MFC (methanol supplemented 100% NMS media; pH 7.2), TY-MFC (undefined LB media containing 50% NMS and 50% LB; pH 7.2) and abiotic MFC. –●– – power densities (CH_3OH-MFC); –●– – power densities (TY-MFC); –●– – power densities (abiotic control); –▲– – voltage (CH_3OH-MFC); –▲– – voltage (TY-MFC); –▲– – voltage (abiotic control).

was 54% higher compared with TY-MFC (50 mW/m^2). The peak current density in CH_3OH-MFC (781 mA/m^2) was ~4.2-fold higher compared with TY-MFC (185 mA/m^2) (Figure S2). The higher activation losses and larger over potential losses limited the power output in TY-MFC. The power output in CH_3OH-MFC (76 mW/m^2) was better than that of the alcohol MFCs reported in earlier studies (40 mW/m^2) [25]. As discussed in the later section, the enhanced performance of CH_3OH-MFC is due to the syntrophic cooperation among diverse bacterial and archaeal members in the consortia (Details in Section 3.3).

The CH_3OH-MFC achieved 23% COD removal efficiency during 25 days of the closed-circuit operations (Figure S4). The internal resistance, an important parameter which determines the fuel cell performance was evaluated using the EIS analysis. The Nyquist plot for the CH_3OH-MFC (Fig. 2a) displayed a smaller semicircle compared with TY-MFC. The diameter of the semicircle in a Nyquist plot is directly proportional to charge transfer resistance at the anode interface in MFCs. To quantify various resistances, the Nyquist data from both CH_3OH-MFC and TY-MFC were fitted to an electrical equivalent circuit (Fig. 2b).

The EEC consisted of biofilm resistance (R_{film}), charge transfer resistance (R_{ct}), Warburg impedance (W) and solution resistance (R_{ohm}). The internal resistance offered by the biofilm (R_{film}) in the CH_3OH-MFC (1.32 kΩ.cm^2) was 46% lower compared with TY-MFC (1.93 kΩ. cm^2) (Fig. 2a, Table 1). The lower value of R_{film} in the CH_3OH-MFC implies the enhanced bioelectrocatalytic ability of the consortia, i.e., the ability to oxidize methanol and transfer the electrons to the anode surface. The lower value of the Bode phase angle maxima in the CH_3OH-MFC (55°) compared with TY-MFC (62°) (Fig. 2b) corroborates that the type of carbon substrate (CH_3OH vs., TY) influences the microbial dynamics in the consortia and its preferential metabolic pathways. The R_{ct} value in the CH_3OH-MFC was extremely low (1.4×10^{-9} kΩ. cm^2) compared with TY-MFC (0.065 kΩ. cm^2). The lower the R_{ct} the better is the electroactive characteristics of the biofilm on the anode surface [26,27]. The above results corroborate with the 3D-LSM micrographs and microbial community analysis where the CH_3OH-MFC yielded thicker and electroactive biofilms than TY-MFC (Discussed in section 3.2 and 3.3).

To ascertain the biocatalytic behavior of biofilms in the CH_3OH-MFC, CVs were generated at a scan rate of 10 mv/s. The CVs for both the CH_3OH-MFC and TY-MFC displayed a redox peak at −0.19 mV (vs Ag/AgCl) confirming their biocatalytic activity (Fig. 3). However, the oxidation peak current in the CH_3OH-MFC (0.0014 mA) was 1.5-fold higher compared with TY-MFC (0.0009 mA), suggesting enhanced Faradaic reactions driven CH_3OH oxidation. The oxidation potential in the CV for the CH_3OH-MFC (−0.34 V vs Ag/AgCl) is attributed to CH_3OH oxidation (−0.2 V vs Ag/AgCl), as reported in the previous studies [28].

Table 1
EIS fitting results showing the different resistances in CH_3OH-MFC and TY-MFC used for enriching flowback water. The total resistance of the electrode and electrolyte was found to be 1.4 kΩ cm^2 and 2 kΩ cm^2 in CH_3OH-MFC and TY-MFC experiments respectively.

Resistances[a] (kΩ. cm^2)	CH_3OH-MFC	TY-MFC
R_{ohm}	0.083	0.058
R_{film}	1.32	1.93
R_{ct}	Negligible (1.4×10^{-9})	0.065

[a] R_{ohm} - Solution resistance; R_{film} - charge transfer resistance; R_p - electrode polarization resistance.

3.2. Morphology, viability and thickness of the electrogenic biofilm

We carried out a post-mortem analysis of the graphite felt anode samples that were continuously exposed to 25 days of the phase-3 tests. We did not observe any biofilm on the anode surface in the abiotic control (Fig. 4a). As shown in Fig. 4b and c, both CH_3OH-MFC and TY-MFC yielded densely packed biofilms that were characterized by rod-shaped microorganisms using SEM. These biofilms exhibited an affinity to adhere to the electrode surface, evident from their heterogeneous characteristics and the ability to aggregate and form an extracellular matrix of polysaccharides and proteins. This finding corroborates with the microbial community analysis which revealed that CH_3OH-MFC and TY-MFC were based on ~81% and 68% electrogenic microbes, respectively. However, the degree of electrogenic behavior varies at the species level. This provides preliminary ideas about the versatile behavior of the microbes enriched from the harsh subsurface environments of the fractured Bakken shale. Fluorescence microscopic analysis was carried out to further examine the ability of the consortia to grow into exoelectrogenic biofilm on the anode surfaces.

A LIVE/DEAD staining technique based on SYTO9 and propidium iodide was used to assess and compare the viable fraction of the

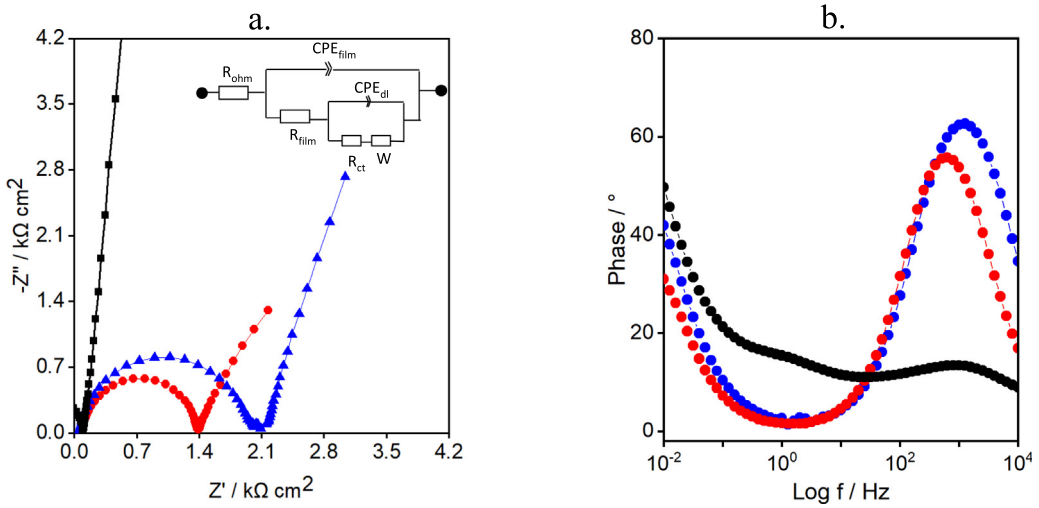

Fig. 2. Electrochemical analysis by EIS. (a) Nyquist plots showing lower internal charge transfer resistance of CH_3OH-MFC compared with TY-MFC. Inset shows the electrical equivalent circuit used for EIS fitting analysis; – CH_3OH-MFC; – TY-MFC; – abiotic control. (b) Bode phase angle plots for CH_3OH-MFC, TY-MFC and abiotic control MFC in the frequency range of 10 MHz to 10 kHz. – CH_3OH-MFC; – TY-MFC; – abiotic control.

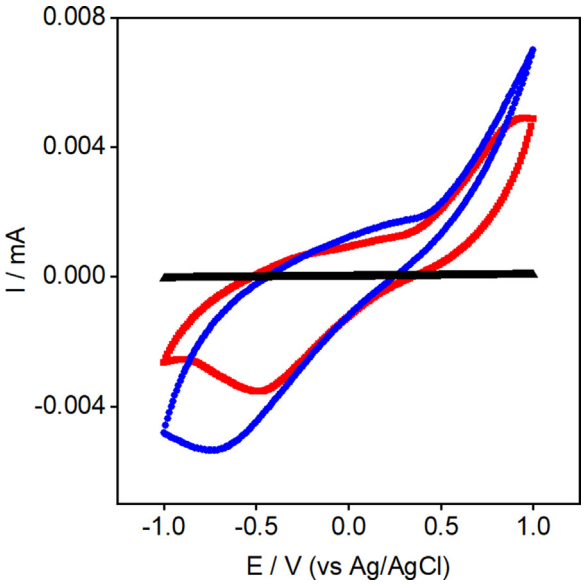

Fig. 3. Electrochemical analysis by CV. Cyclic voltammograms for abiotic control MFC (pH 7.2), CH_3OH-MFC (methanol supplemented 100% NMS media; pH 7.2) and TY-MFC (undefined LB media containing 50% NMS and 50% LB; pH 7.2) on day 25 (scan rate 10 mv/s, potentials between − 0.1 and +0.1 V for carbon felt electrodes vs. the Ag/AgCl reference electrode). —■— – CH_3OH-MFC; —●— – TY-MFC; —▲— – abiotic control.

cells in the biofilm. The abiotic control did not display any fluorescence (Fig. 4d). However, green fluorescence was displayed by both CH_3OH-MFC (83%) and TY-MFC (86%) (Fig. 4e and f). In general methanol substrates (ΔG^O = 37.51 KJ/e^- eq; pH = 7.0) yield lower energy for biological systems compared with glucose (ΔG^O = −41.96 KJ/e^- eq; pH = 7.0) and protein substrates (ΔG^O = −41.96 KJ/e^- eq; pH = 7.0). Although one can expect TY-MFC to yield thicker biofilms, we observed thicker biofilms in CH_3OH-MFC. As shown in the 3D-LSM micrographs, CH_3OH-MFC yielded a 2.7-fold thicker biofilm (83.3 ± 4 μm) compared with TY-MFC (30.6 ± 1.2 μm) (Figure S5). However, these values of the biofilm thicknesses fall within the range (30–85 μm) reported by other MFC researchers [29–31]. We attribute the thicker biofilms (Figure S5) to be responsible for the lower impedance and higher power output in CH_3OH-MFC (Table 1, Fig. 1).

After establishing the higher electrochemical power output in CH_3OH-MFC, we deduce that the methanol substrates (versus TY) allowed the consortia to evolve into a syntrophic group of microorganisms that drove the methanol oxidation (discussed in Section 3.3). The higher biofilm thickness in CH_3OH-MFC is due to the larger percentage of electrogens compared with TY-MFC (Discussed in Section 3.3). Such microorganisms offer lower transmembrane cytochrome activity on the outer biofilm and higher affinity to respire using the solid electrodes [32–34].

3.3. Community analysis of the consortia in CH_3OH-MFC and TY-MFC

Figs. 5 and 6 compares the relative taxonomic abundance of the 16S rRNA gene sequences at a class level and genus level, respectively. The community structure in the CH_3OH-MFC was different compared with TY-MFC. Although both the MFCs yielded a mixture of aerobes and anaerobes, their composition differed at the class level and order level. The taxonomic abundance of the consortia in CH_3OH-MFC was uniquely dominated by methylotrophic community. The percentage of the electrogenic microbes in the CH_3OH-MFC (81%) was higher compared with TY-MFC (68%) (Details in Table 2). This analysis is based on the previously reported electrogenic capabilities of the microbes observed in the consortia (Table 2). Nearly, 91% of the archaeal communities in CH_3OH-MFC have been reported to exhibit electrogenic characteristics. TY-MFC did not yield any detectable levels of the archaeal population.

Genus level microbial community analysis revealed that bacterial population in the CH_3OH-MFC were based on 38% *β-proteobacteria*, 30% *α-proteobacteria*, 21% *γ-proteobacteria* and 11% *Bacteroidetes*. Among *α-proteobacteria*, 29% of the reads mapped *Rhodobacter* that has been recently reported to generate electricity in MFCs [35] and 1% *Rhizobiales*. A recent study corroborates our finding that the flowback water from Bakken Shale consists of microorganisms from *α-proteobacteria* (15–61%), *Δ-proteobacteria* (29–76%), *Firmicutes* (22–37%), *Bacteroidetes* (9–14%) and *Methanobrevibacter* (99% among archaea) [9]. The paragraph below discusses the role of species from *proteobacteria (α, β and γ)* and *Bacterioidia* towards methanol assimilation and electricity generation in CH_3OH-MFC. The flowback water from Marcellus Shale has also been reported to contain *γ-proteobacteria* (6–52%) and *α-proteobacteria* (2–81%), among which *Rhodobacterales* order (*α-proteobacteria*) were dominated to about 68–88% [36].

Recent studies suggest that the microbial communities in the produced water from fractured gas well contain *γ-proteobacteria* (41–47%) and *α-proteobacteria* (39–42%). A study based on a fractured oil well in Pennsylvania reported the domination of *Rhodobacterales* (48–64%) among *α-proteobacteria* [6]. It is clear that the *Rhodobacterales* order occurs in flowback water from many Shale plays across the U.S. On the other hand, all of the major players, including *Alcaligenes* (20%) and *Castellaniella* (18%) from *β-proteobacteria* in CH_3OH-MFC have been reported to display electrogenic behavior [37,38]. *Providencia*, a motile bacterium from the *Enterobacteriaceae* family constituted 21% of *γ-proteobacteria* in CH_3OH-MFC. To the best of our knowledge, none of the prior studies have reported the role of *Providencia* in MFC studies.

The archaeal community in CH_3OH-MFC consisted of 73% *Methanobacterium*, 14% *Methanocorpusculum parvum*, 9% *Methanobrevibacter smithii* and 4% *Methanosarcina*. TY-MFC did not yield any archaeal population. The earlier studies have reported that 99% of archaea in the flowback water from Bakken shale were dominated by *Methanobrevibacter* [9]. Among the archaeal population in CH_3OH-MFC, *Methanobacterium* and *Methanosarcina* can convert acetate into methane via hydrogenotrophic methanogenesis (H_2 + CO_2 or H_2 + methanol) and acetoclastic methanogenesis [39]. *Methanosarcina acetivoransis* is the only methanogen that has been reported to use c-type cytochromes and participate in the extracellular electron transfer process [39]. In contrast to the findings from the current study, the archaeal community in flowback water from Marcellus Shale was characterized by *Methanocalculus*, *Methanoplanus, Methanolobus and Methanohalophilus* [5]. The archaeal community in the formation water from Antrim Shale (Michigan Basin) also contained *Methanolobus profundi* and *Methanohalophilus* [40].

Our gas chromatography tests revealed the absence of methane in the headspace of CH_3OH-MFC, confirming the lack of methanogenic activity. However, the archaeal species observed in the enriched consortia (e.g., *Methanobacterium* sp. [41], *Methanosarcina* sp. [42], and *Methanobrevibacter smithii* [43] have been reported to display methylotrophic capabilities. We expect these archaeal members to syntrophically interact with other bacterial members, especially methylotrophs to drive the methanol oxidation.

Microbial communities in TY-MFC were quite different compared with CH_3OH-MFC. They were based on *Actinobacteria* (34.43%), *Bacteroidia* (16.67%), *γ-proteobacteria* (12.43%), *Ruminobacillus* (8.3%) and miscellaneous species including *Negativicutes*, *Δ-proteobacteria*, *ε-proteobacteria*, *Synergistia* and *Lentisphaeria*

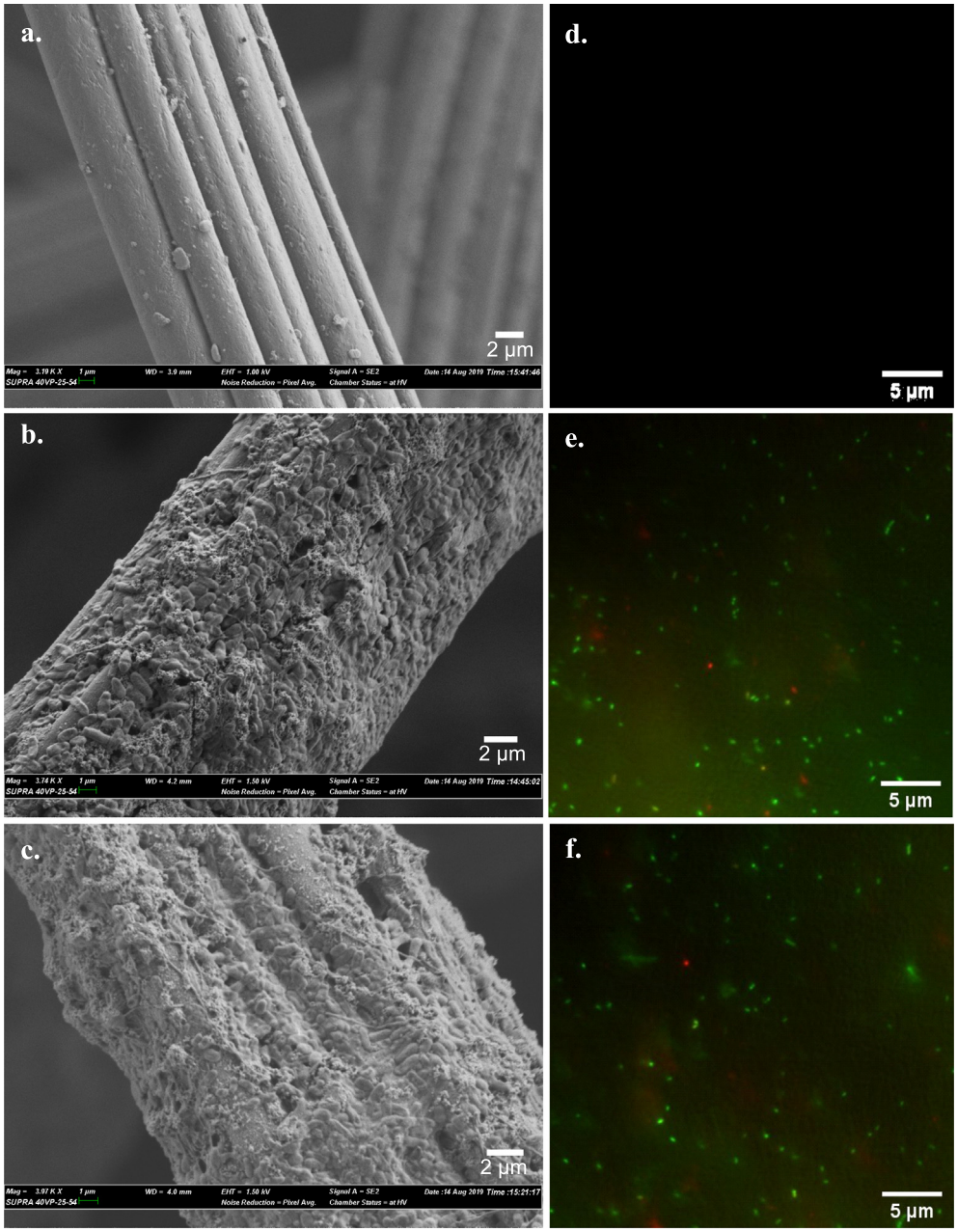

Fig. 4. Electrogenic biofilm morphology by SEM and fluorescence microscopy. (a) abiotic control MFC, (b) CH_3OH-MFC and (c) TY-MFC. SEM micrographs of the anodic biofilm showing the microbial adherence and colonization along with the presence of extracellular matrix. Fluorescent microscopic images of the anodic biofilms stained with Filmtracer™LIVE/DEAD™ Biofilm Viability Kit using SYTO9 (live cells) and propidium iodide stain (dead cells) showing the green and red fluorescence respectively for (d) abiotic control MFC (e) CH_3OH-MFC and (f) TY-MFC. The fluorescent microscopic images suggest that the electrodes of CH_3OH-MFC and TY-MFC were dominated by apparently similar counts of live microbial biota. As expected, the abiotic control MFC did not show any microbial colonization on the electrode surface.

(28.17%). As shown in Table 2, TY-MFC contained a smaller percentage of electrogens compared with CH_3OH-MFC. TY-MFC also did not develop any methylotrophs, and instead yielded *Corynebacterium* sp. that used alcohols, organic acids and sugars prefer as carbon substrates. *Corynebacterium* sp. does not participate in extracellular electron transfer processes [44]. Both CH_3OH-MFC and TY-MFC yielded *Bacteroidia* which represents fermenters that use amino acids, sugars, alcohols and organic acids as carbon substrates [40].

Further studies are warranted to decipher the specific metabolic roles of *Bacteroidetes* in CH_3OH-MFC. Despite the lower degree of microbial diversity, CH_3OH-MFC yielded superior electrical performance compared with TY-MFC. On the other hand, methylotrophs have been reported to use methane, hydrogen and ethanol as electron donors under syntrophic conditions [14,45]. Interestingly, the *Proteobacteria* phylum that dominated CH_3OH-MFC has been reported to display both autotrophic and heterotrophic modes. They have also been widely reported to be involved in a synergistic interaction with other microbial members [15,46,47].

3.4. Electrogenic activity of R. sphaeroides 2.4.1

After establishing that 29% of the bacterial population from *α-proteobacteria* in CH_3OH-MFC mapped *Rhodobacter* and noting that *R. sphaeroides* represents the popular species of *Rhodobacter*, we carried out additional tests to assess the ability of pure

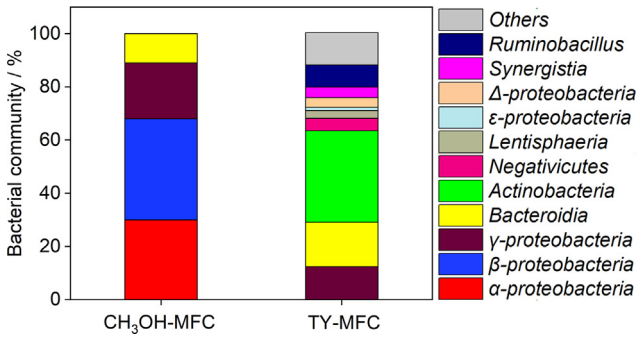

Fig. 5. Class level distribution of flowback water microbial community in CH_3OH-MFC and TY-MFC. Percentage of the bacterial communities of flowback water enriched in CH_3OH-MFC and TY-MFC showing the class level distributions of the bacteria. Others denote sequences that were assigned to unclassified bacteria.

R. sphaeroides to drive CH_3OH-MFC. We used *R. sphaeroides* 2.4.1 as the model strain to explore the methylotrophic ability of *R. sphaeroides* in MFCs solely fed with methanol substrate. *R. sphaeroides* did not yield any significant electrical power output when CH_3OH-MFC tests were carried out under dark conditions. However, we noticed a significant boost in the performance of CH_3OH-MFC when the tests were repeated in the presence of the white light (a photo-heterotrophic mode). The extensive electrochemical tests based on polarization curves and EIS analysis revealed the electrogenic nature of *R. spaeroides* 2.4.1. Results showed that *R. sphaeroides* yielded 5.4-fold higher power densities on Day 25 (13 mW/m^2) compared with Day 1 (2.4 mW/m^2) (Fig. 7a). Nyquist plots revealed that the total resistance (13.4 $k\Omega\ cm^2$) on Day 25 was 25% lower compared with that on Day 1 (21.1 $k\Omega\ cm^2$) (Fig. 7b, c and Table 3). This result implies that the growth of *R. sphaeroides* biofilm was responsible for the decreasing polarization resistance and the increasing bioelectrochemical kinetics of the methanol oxidation.

CH_3OH-MFC based on the pure cultures of *R. sphaeroides* achieved 86% COD removal efficiency (COD_i = 1227 mg/L and COD_f = 177 mg/L) during 25 days of the closed-circuit operation. Considering the consistent electrochemical power output of CH_3OH-MFC using methanol as the sole carbon source, we attribute the bioelectrochemical processes to be a primary sink for the COD. We also do not suspect that the volatilization processes resulted in COD removal. The domination of the bioelectrochemical oxidation pathway is evident from the rampant growth of biofilms on the anode surface in CH_3OH-MFC solely fed with methanol (Details in Section 3.2). These results corroborate the ability of *R. sphaeroides* to convert methanol substrates into electricity, a finding consistent from that of our earlier study [59]. The performance of CH_3OH-MFCs could be further enhanced by optimizing the MFC architecture, for example by replacing the typical carbon electrodes with superconducting metal electrodes [59].

To further ascertain that the electric current is solely generated by the methanol oxidation reaction, we carried out following additional three MFC tests: (i) pure cultures of *R. sphaerodies* containing NMS media with methanol and inoculum (CH_3OH^+ RSP^+-MFC), (ii) NMS media with methanol without inoculum (CH_3OH^+ RSP^--MFC), and (iii) NMS media without methanol and inoculum (CH_3OH^-

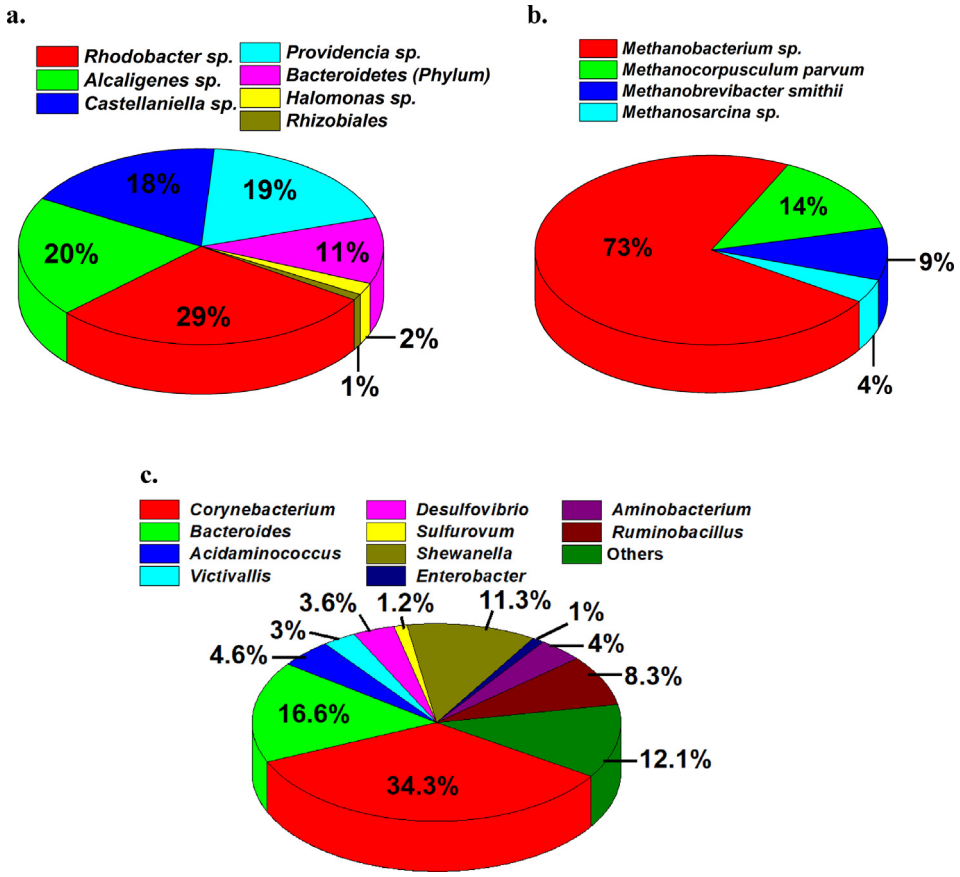

Fig. 6. Genus level distribution of flowback water microbial community in CH_3OH-MFC and TY-MFC. (a and b) The relative taxonomic abundance of the 16S rRNA gene sequences of the flow back water enriched in CH_3OH-MFC showing the bacterial and archaeal communities. (c) The relative taxonomic abundance of bacterial population of TY-MFC, wherein the archaea were found to be at the undetectable levels in the DNA. Gene sequences were run through USEARCH global search alignment algorithm along with a Python program to identify the actual taxonomic assignment. Others denote sequences that were assigned to the unclassified bacteria.

Table 2
Possible electrogenic behavior of the enriched microbial consortia from CH_3OH-MFC and TY-MFC. Electrogenic capability comparison was based on the previously reported exoelectrogenic capabilities of each microbe. * Microbes for which species-level identification is rarely reported for exoelectrogenic activity.

Class of bacteria	Bacteria	MFCs	Electrogenic behavior	% Composition	References
		The bacterial community in CH_3OH-MFC and TY-MFC			
α-proteobacteria	*R. sphaeroides*	CH_3OH-MFC	Yes	29	[35]
	Rhizobiales *	CH_3OH-MFC	Yes	1	[48]
β-proteobacteria	*Alcaligenes faecalis*	CH_3OH-MFC	Yes	20	[38]
	Castellaniella defragrans	CH_3OH-MFC	Yes	18	[37]
γ-proteobacteria	*Providencia* sp.*	CH_3OH-MFC	No	19	–
	Halomonas sp.*	CH_3OH-MFC	Yes	2	[49]
	Shewanella oneidensis	TY-MFC	Yes	11.38	[50]
	Enterobacter ludwigii	TY-MFC	Yes	1.05	[51]
Δ-proteobacteria	*Desulfovibrio* sp.*	TY-MFC	Yes	3.68	[52]
ε-proteobacteria	*Sulfurovum* sp.*	TY-MFC	Yes	1.15	[53]
Actinobacteria	*Corynebacterium humireducens*	TY-MFC	Yes	34.43	[44,54]
Bacteroidia	*Bacteroidia (class)*	CH_3OH-MFC	Yes	11	[55]
Bacteroidia	*Bacteroidia (class)*	TY-MFC	Yes	16.67	[55]
Negativicutes	*Acidaminococcus* sp.*	TY-MFC	No	4.63	–
Lentisphaeria	*Victivallis* sp.*	TY-MFC	Yes	2.96	[56]
Synergistia	*Aminobacterium* sp.*	TY-MFC	No	3.98	–
Ruminobacillus	Unclassified	TY-MFC	No	8.31	–
Others	Unclassified	TY-MFC	–	12.15	–
		The archaeal community in CH_3OH-MFC			
Methanobacteria	*Methanobacterium* sp.*	CH_3OH-MFC	Yes	73	[57]
Methanomicrobia	*Methanocorpusculum parvum*	CH_3OH-MFC	Yes	14	[58]
Methanobacteria	*Methanobrevibacter smithii*	CH_3OH-MFC	No	9	–
Methanomicrobia	*Methanosarcina acetivorans*	CH_3OH-MFC	Yes	4	[58]

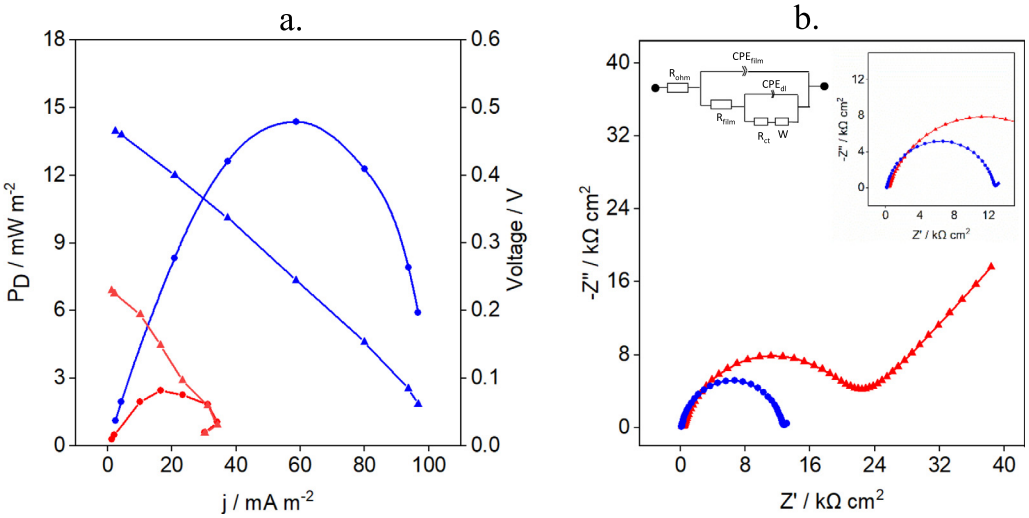

Fig. 7. Electrochemical performances of *R. sphaeroides* pure cultures. (a). Comparison of power densities of *R. sphaeroides* pure cultures in CH_3OH-MFC during Day 1 and Day 25; –●– – power densities (Day 1); –●– – power densities (Day 25); –▲– – Voltage (Day 1); –▲– – Voltage (Day 25). (b). Nyquist plots of CH_3OH-MFC showing lower charge transfer resistance during Day 25 than Day 1 revealing the pure cultures could oxide methanol efficiently thereby forming a biofilm on the anode for extracellular electron transfer. Inset shows the electrical equivalent circuit used for EIS fitting analysis; –▲– – Day 1; –●– – Day 25.

Table 3
EIS fitting results showing the different resistances in CH_3OH-MFC using *R. sphaeroides* pure cultures grown in NMS media with methanol as an electron donor. The total resistance of the electrode and electrolyte was found to be 21.1 kΩ cm^2 and 13.4 kΩ cm^2 during Day 1 and Day 25 of the CH_3OH-MFC experiments.

Resistances[a] (kΩ. cm^2)	Day 1	Day 25
R_{ohm}	Negligible (5.6×10^{-7})	0.128
R_{film}	0.405	12.73
R_{ct}	20.75	0.458

[a] R_{ohm} - Solution resistance; R_{film} - charge transfer resistance; R_p - electrode polarization resistance.

RSP⁻-MFC), all under photoheterotrophic growth mode. The current (i) vs. time (t) plot showed that CH_3OH^+ RSP^+-MFC yielded higher current (770 μA under 500 Ω external resistance) while CH_3OH^+ RSP^--MFC and CH_3OH^- RSP^--MFC did not register any current (Figure S6a). CH_3OH^+ RSP^+-MFC yielded peak power density of 8.6 mW/m^2 whereas CH_3OH^+ RSP^--MFC and CH_3OH^- RSP^--MFC did not register any significant power outputs (Figure S6c). The EIS analysis based on the data from the Nyquist plots (Figure S6b) showed that the charge transfer resistance of the biofilm (R_{film} = 0.473 kΩ.cm^2) was lower in CH_3OH^+ RSP^+-MFC) compared with CH_3OH^+ RSP^--MFC (1.98 kΩ.cm^2) and CH_3OH^- RSP^-MFC (3.324 kΩ.cm^2). CH_3OH^+ RSP^+-MFC showed 4-fold and 7-fold lower charge transfer resistances compared with CH_3OH^+ RSP^--MFC and CH_3OH^- RSP^-MFC, respectively. CH_3OH^+ RSP^+-MFC also offered higher coulombic efficiency (20%) compared with CH_3OH^+ RSP^--MFC (0.17×10^{-7}%). This result revealed that CH_3OH^+ RSP^+-MFC yields higher performance, based on the polarization data and impedance analysis (Figure S6).

The above results confirm that the electric current in CH_3OH^+ RSP^+-MFC is solely due to methanol oxidation. These results also confirm that *R. sphaeroides* play a key contribution to high COD removal efficiency (86%) in CH_3OH^+ RSP^+-MFC (after 25 days of closed-circuit conditions). Methanol oxidation in *R. sphaeroides* typically involves a series of cascaded oxidation products including formaldehyde, formate and carbon dioxide, primarily based on crucial genes including PQQ dependent methanol dehydrogenase, formaldehyde dehydrogenase and formate dehydrogenase [60].

The electrogenic capacities of *R. sphaeroides* are highly dependent on the carbon substrate used and *R. sphaeroides* could generate current from a variety of carbon substrates including lactate, malate, butyrate, glucose, fumarate, peptone and yeast extract under photosynthetic conditions [61]. These results corroborate with the previous reports of *R. sphaeroides* yielding electrons under light irradiation with various electron donors including acetate [35], succinate [61], and propionate [62]. In a recent study, we reported that metal electrodes can be used to enhance the growth of *R. sphaeroides* biofilms in MFCs [63].

3.5. Potential pathways used by the consortia to generate electricity from methanol

As depicted in Scheme 1 and discussed below, the methanol oxidation in CH_3OH-MFC is driven by the syntrophic interactions between methanogens, acetogens and hydrogenogens [64]. *R. sphaeroides* oxidize CH_3OH into formaldehyde using a gene regulatory network involving pyrroloquinoline quinone dependent dehydrogenase (*XoxF*) and periplasmic c-type cytochromes (*CycB* -a cyt c_{553i} homolog) genes for methanol-dependent oxygen uptake [60]. The co-existence of methanogens and methylotrophs allowed the removal of toxic formaldehyde from the CH_3OH-MFC [65]. Such syntrophic cooperation between methanotrophs and methanogens has also been reported for indigenous microbial communities in the Marcellus Shale [66]. Syntrophic interactions of a facultative methylotroph *Methyloceanibacter caenitepidi* Gela4 and methanotroph *Methylocaldum marinum* S8 revealed that acetate could be a major carbon source than methanol for *M. caenitepidi* Gela4 [67]. A series of these co-existence studies are needed to reveal precisely the methanol-independent cross-feeding mechanism among methanotrophs and non-methanotrophs. Formaldehyde can be further oxidized to formate by glutathione-dependent formaldehyde dehydrogenase (GSH-FDH) which is then oxidized to CO_2 and electrons using formate dehydrogenase [60]. Also, *R. sphaeroides* produces an acyl-homoserine lactone (AHL) molecules called 7,8-*cis*-N-(tetradecenoyl) homoserine lactone which is involved in quorum sensing (QS) signaling pathway. This QS pathway allows the bacterial species to activate a specific set of signaling proteins i.e., community escape response proteins (*cerA* and *cerI*) at a threshold population density [68]. Other than that, *R. sphaeroides* harbors well-characterized genes encoding for cytochrome *c* oxidase (GeneID:3719145), exopolysaccharide production protein (GeneID:3720181), pili assembly protein (GeneID:3719188), flagellar protein (GeneID:3720115), all of which influence biofilm formation and extracellular electron transfer process. These in turn activate the intrinsic properties of electroactive biofilms [69]. Also, the quorum sensing mechanism which has been well established in *Shewanella oneidensis;* here *LuxS* gene is involved in metabolizing the AHL synthesis that influences biofilm formation [70].

On the other hand, yeast extract contains flavin-like molecules that serve as redox species to promote the performance of MFCs [71,72]. Interestingly, TY-MFC displayed inferior performance compared with CH_3OH-MFC (Figs. 1–3). TY-MFC contained yeast extract while CH_3OH-MFC was devoid of exogenous mediators. *Corynebacterium* sp., a predominant bacterial member in TY-MFC relies upon mediated electron transfer (MET) processes [44], reducing overall electrochemical power output. In contrast, *R. sphaeroides* a dominant member in CH_3OH-MFC secretes the QS signaling molecules, regulates bio-electrochemical activities, and enables the growth of electroactive biofilms [73,74]. Moreover, a mixed consortium of acidogenic and methanogenic bacteria yields

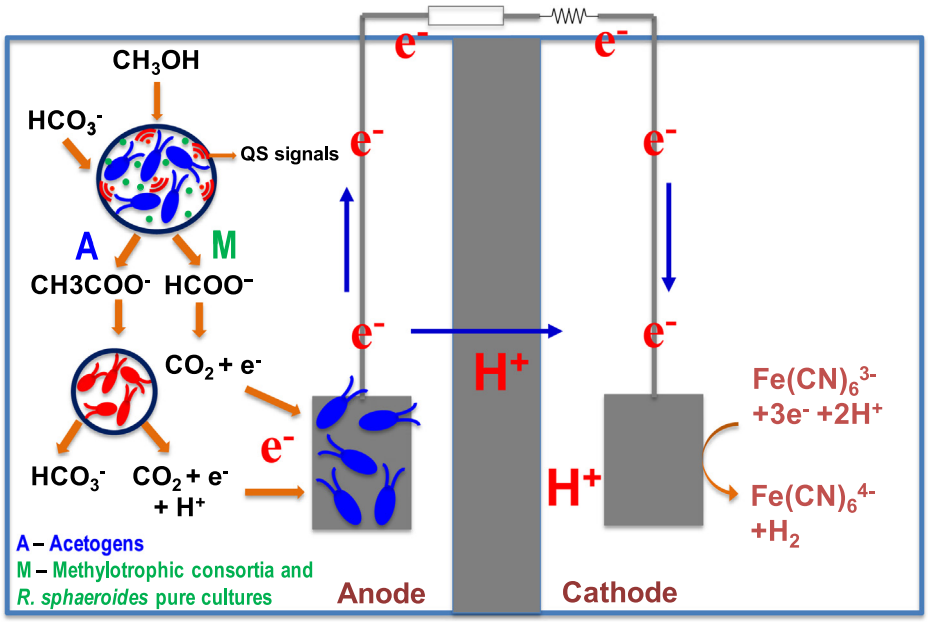

Scheme 1. Proposed mechanism of methanol oxidation and current flow from CH_3OH-MFC used in this study. Methanol is oxidized to carbon dioxide and electrons by the syntrophic interactions of methylotrophic and acetogenic consortia in the anodic compartment. Also, the quorum-sensing pathway of *R. sphaeroides* synthesizes novel homoserine lactone signal (autoinducers), 7,8-*cis*-N-(tetradecenoyl) homoserine lactone that enhances the intrinsic properties of electroactive biofilm formation. Electrons generated from acetogenic and methylotrophic pathways sink towards the electrodes which are attributed by exopolysaccharide secretion and thick biofilm formation. The electrons will then be transferred through the external circuit to the cathode wherein potassium ferricyanide was reduced to potassium ferrocyanide occurs. M - methylotrophic bacteria; A - acetogenic bacteria; ((•)) – quorum sensing (QS) signals; ● – autoinducer molecules.

acids (acetate/butyrate) per unit methanol converted [64]. This is evident from the presence of *Methanosarcina* sp. a methanol utilizing methanogen that can oxidize methanol to bicarbonate. We speculate that syntrophic cooperation between CH_3OH-utilizing acetogens and methylotrophs drive acetogenic fermentation of CH_3OH. This explains the higher electrical performance of CH_3-OH-MFC. On the other hand, the presence of sulfate-reducing bacteria in TY-MFC could inhibit the acetogenic fermentation due to the formation of sulfides. Noting that the headspace of CH_3OH-MFCs did not register any detectable levels of methane, we rule out the possibility of methanogenic activity. We also did not observe any methane-oxidizing bacteria in the consortia.

We expect the reaction intermediates of the methylotrophic pathway and acetogenic pathways to yield volatile fatty acids [75] which can be utilized as carbon sources by methylotrophs listed in Table 2. This result corroborates with the previous finding related to inhibitory effects of sulfides on methanol oxidation by a co-culture of *Acetobacterium woodii*, *Sporomusa ovata* and *Desulfovibrio vulgaris* [64]. This result supports our hypothesis on the syntrophic interactions between acetogenic and methylotrophic communities. Similar syntrophic interactions have been reported for the microbial consortia involved in the bioremediation of vanadium [45] and chromium [76,77] from wastewater. Another relevant example is the coexistence of *Geobacter* sp. (bacteria) and *Methanobacterium* sp. (archaea) that jointly facilitated the extracellular electron transfer to electrodes [78]. Aerobic methylotrophs have also been reported to be beneficial to consume oxygen that may leak inadvertently into the anode chamber [79,80]. The current study revealed potential syntrophic cooperation among *R. sphaeroides*, *Alcaligenes* and *Castellaniella* to sustain anaerobic bioconversion of methanol into electricity in CH_3OH-MFC.

3.6. Conclusions

The current study identified and enriched the electrogenic methylotrophic consortia from flowback water for microbial fuel cell applications. The enriched consortia that contained species from α-*proteobacteria*, β-*proteobacteria*, γ-*proteobacteria* and *Bacteroidia* was found to be effective in generating electricity from methanol under ambient conditions. Among these community members, *R. sphaeroides* widely exists in many shale extractions sites. The electrogenic activity of a pure culture of *R. sphaeroides* 2.4.1. was also established in this study. A series of metabolic pathway reconstruction studies revealing the gene regulatory networks will enable better assimilation of methanol by methylotrophs under stressful anaerobic conditions. Metagenomic and metatranscriptomic analysis is also needed to analyze the gene expression profiling of candidate genes involved in catabolic pathways.

In conclusion, the indigenous methylotrophs can be used to develop passive treatment technologies for selectively treating methanol and potentially methane compounds in the flowback water.

Declaration of Competing Interest

The authors declare that they have no known competing financial interests or personal relationships that could have appeared to influence the work reported in this paper.

Acknowledgments

Gadhamshetty acknowledges the funding support from the Electric Power Research Institute (# 10003325), NASA (# NNX16AQ98A), and National Science Foundation BuGReMeDEE Award (# 1736255). We thank the editor and reviewers for the thoughtful comments.

Appendix A. Supplementary material

Supplementary data to this article can be found online at https://doi.org/10.1016/j.bioelechem.2020.107549.

References

[1] S. Gaswirth, K. Marra, T. Cook, R.R. Charpentier, D.L. Gautier, D.K. Higley, T.R. Klett, M.D. Lewan, P.G. Lillis, C.J. Schenk, M.E. Tennyson, K.J. Whidden, Assessment of undiscovered oil resources in the Bakken and Three Forks formations, Williston Basin Province, Montana, North Dakota, and South Dakota, USGS Fact Sheet (2013) 1–4. http://pubs.usgs.gov/fs/2013/3013/fs2013-3013.pdf.

[2] N. Shrestha, G. Chilkoor, J. Wilder, V. Gadhamshetty, J.J. Stone, Potential water resource impacts of hydraulic fracturing from unconventional oil production in the Bakken shale, Water Res. 108 (2017) 1–24, https://doi.org/10.1016/j.watres.2016.11.006.

[3] G. Chilkoor, N. Shrestha, D. Soeder, V. Gadhamshetty, Corrosion and environmental impacts during the flowback water disposal associated with the Bakken shale, Corros. Sci. 133 (2018) 48–60, https://doi.org/10.1016/j.corsci.2018.01.019.

[4] V. Gadhamshetty, N. Shrestha, G. Chilkoor, J.R. Bathi, Emerging environmental impacts of unconventional oil development in the Bakken formation in the Williston Basin of Western North Dakota. In: Drogos, D.L. (Ed.), Hydraulic Fracturing: Environmental Issues., in: Am. Chem. Soc. Washington, DC, 2015.

[5] A. Murali Mohan, A. Hartsock, R.W. Hammack, R.D. Vidic, K.B. Gregory, Microbial communities in flowback water impoundments from hydraulic fracturing for recovery of shale gas, FEMS Microbiol. Ecol. 86 (2013) 567–580, https://doi.org/10.1111/1574-6941.12183.

[6] A. Murali Mohan, A. Hartsock, K.J. Bibby, R.W. Hammack, R.D. Vidic, K.B. Gregory, Microbial community changes in hydraulic fracturing fluids and produced water from shale gas extraction, Environ. Sci. Technol. 47 (2013) 13141–13150, https://doi.org/10.1021/es402928b.

[7] Krzmarzick M.J., McCutchan A., Carroll J., T. Lozano, Microbial enrichment from six hydraulic fracturing fluids and biogeochemical characteristics of flowback waters in Oklahoma shale formations, in: Am. Geophys. Union, Fall Meet., 2017: p. Abstract #B11B-1669.

[8] T.M. Lozano, A.L. McCutchan, M.J. Krzmarzick, Hydraulic fracturing fluid compositions induce differential enrichment of soil bacterial communities, Environ. Eng. Sci. 36 (2019) 385–395, https://doi.org/10.1089/ees.2018.0271.

[9] Wang H., Lu L., Chen X., Bian Y., Ren Z.J., Geochemical and microbial characterizations of flowback and produced water in three shale oil and gas plays in the central and western United States, Water Res. 164 (2019) 1 – 11, https://doi.org/10.1016/j.watres.2019.114942 114942.

[10] A. Butkovskyi, H. Bruning, S.A.E. Kools, H.H.M. Rijnaarts, A.P. Van Wezel, Organic pollutants in Shale Gas flowback and produced waters: identification, potential ecological impact, and implications for treatment strategies, Environ. Sci. Technol. 51 (2017) 4740–4754, https://doi.org/10.1021/acs.est.6b05640.

[11] Y. Morono, J.R. Wishart, M. Ito, A. Ijiri, T. Hoshino, M. Torres, C. Verba, T. Terada, F. Inagaki, F.S. Colwell, Microbial metabolism and community dynamics in hydraulic fracturing fluids recovered from deep hydrocarbon-rich shale, Front. Microbiol. 10 (2019) 1–14, https://doi.org/10.3389/fmicb.2019.00376.

[12] C.G. Struchtemeyer, M.S. Elshahed, Bacterial communities associated with hydraulic fracturing fluids in thermogenic natural gas wells in North Central Texas, USA, FEMS Microbiol. Ecol. 81 (2012) 13–25, https://doi.org/10.1111/j.1574-6941.2011.01196.x.

[13] S. Radajewski, G. Webster, D.S. Reay, S.A. Morris, P. Ineson, B.B. Nedwell, J.I. Prosser, J.C. Murrell, Identification of active methylotroph populations in an acidic forest soil by stable-isotope probing, Microbiology 148 (2002) 2331–2342, https://doi.org/10.1099/00221287-148-8-2331.

[14] Y. Jiang, B. Zhang, C. He, J. Shi, A.G.L. Borthwick, X. Huang, Synchronous microbial vanadium (V) reduction and denitrification in groundwater using hydrogen as the sole electron donor, Water Res. 141 (2018) 289–296, https://doi.org/10.1016/j.watres.2018.05.033.

[15] B. Zhang, Y. Jiang, K. Zuo, C. He, Y. Dai, Z.J. Ren, Microbial vanadate and nitrate reductions coupled with anaerobic methane oxidation in groundwater, J. Hazard. Mater. 382 (2020), https://doi.org/10.1016/j.jhazmat.2019.121228 121228.

[16] V. Baytshtok, H. Lu, H. Park, S. Kim, R. Yu, K. Chandran, Impact of varying electron donors on the molecular microbial ecology and biokinetics of methylotrophic denitrifying bacteria, Biotechnol. Bioeng. 102 (2009) 1527–1536, https://doi.org/10.1002/bit.22213.

[17] O. Monzon, Y. Yang, J. Kim, A. Heldenbrand, Q. Li, P.J.J. Alvarez, Microbial fuel cell fed by Barnett Shale produced water: Power production by hypersaline autochthonous bacteria and coupling to a desalination unit, Biochem. Eng. J. 117 (2017) 87–91, https://doi.org/10.1016/j.bej.2016.09.013.

[18] B. Zhang, H. Zhao, S. Zhou, C. Shi, C. Wang, J. Ni, A novel UASB-MFC-BAF integrated system for high strength molasses wastewater treatment and bioelectricity generation, Bioresour. Technol. 100 (2009) 5687–5693, https://doi.org/10.1016/j.biortech.2009.06.045.

[19] B. Zhang, C. Feng, J. Ni, J. Zhang, W. Huang, Simultaneous reduction of vanadium (V) and chromium (VI) with enhanced energy recovery based on microbial fuel cell technology, J. Power Sources. 204 (2012) 34–39, https://doi.org/10.1016/j.jpowsour.2012.01.013.

[20] J. Zhang, B. Zhang, C. Tian, Z. Ye, Y. Liu, Z. Lei, W. Huang, C. Feng, Simultaneous sulfide removal and electricity generation with corn stover biomass as co-substrate in microbial fuel cells, Bioresour. Technol. 138 (2013) 198–203, https://doi.org/10.1016/j.biortech.2013.03.167.

[21] N. Shrestha, G. Chilkoor, J. Wilder, Z.J. Ren, V. Gadhamshetty, Comparative performances of microbial capacitive deionization cell and microbial fuel cell fed with produced water from the Bakken shale, Bioelectrochemistry 121 (2018) 56–64, https://doi.org/10.1016/j.bioelechem.2018.01.004.

[22] B. Akyon, E. Stachler, N. Wei, K. Bibby, Microbial mats as a biological treatment approach for saline wastewaters: The case of produced water from hydraulic fracturing, Environ. Sci. Technol. 49 (2015) 6172–6180, https://doi.org/10.1021/es505142t.

[23] S.N. Dedysh, A. Didriksen, O.V. Danilova, S.E. Belova, S. Liebner, M.M. Svenning, *Methylocapsa palsarum* sp. nov., a methanotroph isolated from a subarctic discontinuous permafrost ecosystem, Int. J. Syst. Evol. Microbiol. 65 (2015) 3618–3624, https://doi.org/10.1099/ijsem.0.000465.

[24] H. Luo, P. Xu, T.M. Roane, P.E. Jenkins, Z. Ren, Microbial desalination cells for improved performance in wastewater treatment, electricity production, and desalination, Bioresour. Technol. 105 (2012) 60–66, https://doi.org/10.1016/j.biortech.2011.11.098.

[25] J.R. Kim, S.H. Jung, J.M. Regan, B.E. Logan, Electricity generation and microbial community analysis of alcohol powered microbial fuel cells, Bioresour. Technol. 98 (2007) 2568–2577, https://doi.org/10.1016/j.biortech.2006.09.036.

[26] S. Gupta, A. Yadav, S. Singh, N. Verma, Synthesis of silicon carbide-derived carbon as an electrode of a microbial fuel cell and an adsorbent of aqueous Cr (VI), Ind. Eng. Chem. Res. 56 (2017) 1233–1244, https://doi.org/10.1021/acs.iecr.6b03832.

[27] E. Taşkan, S. Bulak, B. Taşkan, M. Şaşmaz, S. El Abed, A. El Abed, Nitinol as a suitable anode material for electricity generation in microbial fuel cells, Bioelectrochemistry 128 (2019) 118–125, https://doi.org/10.1016/j.bioelechem.2019.03.008.

[28] C. Anthony, Bacterial Oxidation of Methane and Methanol, Adv. Microb. Physiol. 27 (1986) 113–210, https://doi.org/10.1016/S0065-2911(08)60305-7.

[29] K.P. Nevin, H. Richter, S.F. Covalla, J.P. Johnson, T.L. Woodard, A.L. Orloff, H. Jia, M. Zhang, D.R. Lovley, Power output and columbic efficiencies from biofilms of *Geobacter sulfurreducens* comparable to mixed community microbial fuel cells, Environ. Microbiol. 10 (2008) 2505–2514, https://doi.org/10.1111/j.1462-2920.2008.01675.x.

[30] M. Schechter, A. Schechter, S. Rozenfeld, E. Efrat, R. Cahan, Anode Biofilm, Technology and Application of Microbial Fuel Cells, Chin-Tsan Wang, IntechOpen (2014), https://doi.org/10.5772/58432. https://www.intechopen.com/books/technology-and-application-of-microbial-fuel-cells/anode-biofilm.

[31] B. Saba, A.D. Christy, Z. Yu, A.C. Co, R. Islam, O.H. Tuovinen, Characterization and performance of anodic mixed culture biofilms in submersed microbial fuel cells, Bioelectrochemistry 113 (2017) 79–84, https://doi.org/10.1016/j.bioelechem.2016.10.003.

[32] S.M. Strycharz-Glaven, R.M. Snider, A. Guiseppi-Elie, L.M. Tender, On the electrical conductivity of microbial nanowires and biofilms, Energy Environ. Sci. 4 (2011) 4366–4379, https://doi.org/10.1039/c1ee01753e.

[33] H. Liu, S. Cheng, B.E. Logan, Power generation in fed-batch microbial fuel cells as a function of ionic strength, temperature, and reactor configuration, Environ. Sci. Technol. 39 (2005) 5488–5493, https://doi.org/10.1021/es050316c.

[34] C.I. Torres, A.K. Marcus, H.S. Lee, P. Parameswaran, R. Krajmalnik-Brown, B.E. Rittmann, A kinetic perspective on extracellular electron transfer by anode-respiring bacteria, FEMS Microbiol. Rev. 34 (2010) 3–17, https://doi.org/10.1111/j.1574-6976.2009.00191.x.

[35] B.H. Cadirci, An electricity production study by *Rhodobacter sphaeroides*, Int. J. Hydrogen Energy. 43 (2018) 18001–18006, https://doi.org/10.1016/j.ijhydene.2018.01.146.

[36] Mohan A.M., Bibby K.J., Lipus D., Hammack R.W., Gregory K.B., The functional potential of microbial communities in hydraulic fracturing source water and produced water from natural gas extraction characterized by metagenomic sequencing , PLoS ONE 9 (2014) 1 – 12), https://doi.org/10.1371/journal.pone.0107682e 107682.

[37] Y. Sun, J. Wei, P. Liang, X. Huang, Electricity generation and microbial community changes in microbial fuel cells packed with different anodic materials, Bioresour. Technol. 102 (2011) 10886–10891, https://doi.org/10.1016/j.biortech.2011.09.038.

[38] X. Wang, P. Yu, C. Zeng, H. Ding, Y. Li, C. Wang, A. Lu, Enhanced *Alcaligenes faecalis* denitrification rate with electrodes as the electron donor, Appl. Environ. Microbiol. 81 (2015) 5387–5394, https://doi.org/10.1128/AEM.00683-15.

[39] C. Welte, U. Deppenmeier, Bioenergetics and anaerobic respiratory chains of aceticlastic methanogens, Biochim. Biophys. Acta - Bioenerg. 2014 (1837) 1130–1147, https://doi.org/10.1016/j.bbabio.2013.12.002.

[40] C. Wuchter, E. Banning, T.J. Mincer, N.J. Drenzek, M.J.L. Coolen, Microbial diversity and methanogenic activity of antrim shale formation waters from recently fractured wells, Front. Microbiol. 4 (2013) 1–14, https://doi.org/10.3389/fmicb.2013.00367.

[41] G. Borrel, K. Joblin, A. Guedon, J. Colombet, V. Tardy, A.C. Lehours, G. Fonty, *Methanobacterium lacus* sp. nov., isolated from the profundal sediment of a freshwater meromictic lake, Int. J. Syst. Evol. Microbiol. 62 (2012) 1625–1629, https://doi.org/10.1099/ijs.0.034538-0.

[42] A. Bose, M.A. Pritchett, W.W. Metcalf, Genetic analysis of the methanol- and methylamine-specific methyltransferase 2 genes of *Methanosarcina acetivorans* C2A, J. Bacteriol. 190 (2008) 4017–4026, https://doi.org/10.1128/JB.00117-08.

[43] B.S. Samuel, E.E. Hansen, J.K. Manchester, P.M. Coutinho, B. Henrissat, R. Fulton, P. Latreille, K. Kim, R.K. Wilson, J.I. Gordon, Genomic and metabolic adaptations of *Methanobrevibacter smithii* to the human gut, Proc. Natl. Acad. Sci. U. S. A. 104 (2007) 10643–10648, https://doi.org/10.1073/pnas.0704189104.

[44] M. Liu, Y. Yuan, L.X. Zhang, L. Zhuang, S.G. Zhou, J.R. Ni, Bioelectricity generation by a Gram-positive *Corynebacterium* sp. strain MFC03 under alkaline condition in microbial fuel cells, Bioresour. Technol. 101 (2010) 1807–1811, https://doi.org/10.1016/j.biortech.2009.10.003.

[45] B. Zhang, R. Qiu, L. Lu, X. Chen, C. He, J. Lu, Z.J. Ren, Autotrophic vanadium (V) bioreduction in groundwater by elemental sulfur and zerovalent iron, Environ. Sci. Technol. 52 (2018) 7434–7442, https://doi.org/10.1021/acs.est.8b01317.

[46] B. Zhang, S. Wang, M. Diao, J. Fu, M. Xie, J. Shi, Z. Liu, Y. Jiang, X. Cao, A.G.L. Borthwick, Microbial community responses to vanadium distributions in mining geological environments and bioremediation assessment, J. Geophys. Res. Biogeosci. 124 (2019) 601–615, https://doi.org/10.1029/2018JG004670.

[47] Zhang B., Cheng Y., Shi J., Xing X., Zhu Y., Xu N., Xia J., Borthwick A.G.L., Insights into interactions between vanadium (V) bio-reduction and pentachlorophenol dechlorination in synthetic groundwater , Chem. Eng. J. 375 (2019) 1 – 9, doi: https://doi.org/10.1016/j.cej.2019.121965 121965.

[48] Zhang P., Yang C., Xu Y., Li H., Shi W., Xie X., Lu M., Huang L., Huang W., Accerelerating the startup of microbial fuel cells by facile microbial acclimation, Bioresour. Technol. Reports. 8 (2019), https://doi.org/10.1016/j.biteb.2019.100347 100347.

[49] L. Rago, P. Cristiani, F. Villa, S. Zecchin, A. Colombo, L. Cavalca, A. Schievano, Influences of dissolved oxygen concentration on biocathodic microbial communities in microbial fuel cells, Bioelectrochemistry 116 (2017) 39–51, https://doi.org/10.1016/j.bioelechem.2017.04.001.

[50] C. Engel, F. Schattenberg, K. Dohnt, U. Schröder, S. Müller, R. Krull, Long-term behavior of defined mixed cultures of *Geobacter sulfurreducens* and *Shewanella oneidensis* in bioelectrochemical systems, Front. Bioeng. Biotechnol. 7 (2019) 1–12, https://doi.org/10.3389/fbioe.2019.00060.

[51] C. Feng, J. Li, D. Qin, L. Chen, F. Zhao, S. Chen, H. Hu, C.P. Yu, Characterization of exoelectrogenic bacteria enterobacter strains isolated from a microbial fuel cell exposed to copper shock load, PLoS ONE 9 (2014) 1–10, https://doi.org/10.1371/journal.pone.0113379.

[52] W. Miran, J. Jang, M. Nawaz, A. Shahzad, S.E. Jeong, C.O. Jeon, S. Lee, Mixed sulfate-reducing bacteria-enriched microbial fuel cells for the treatment of wastewater containing copper, Chemosphere 189 (2017) 134–142. https://doi.org/10.1016/j.chemosphere.2017.09.048.

[53] C.E. Reimers, C. Li, M.F. Graw, P.S. Schrader, M. Wolf, The identification of cable bacteria attached to the anode of a benthic microbial fuel cell: Evidence of long distance extracellular electron transport to electrodes, Front. Microbiol. 8 (2017) 1–14, https://doi.org/10.3389/fmicb.2017.02055.

[54] C.Y. Wu, L. Zhuang, S.G. Zhou, F.B. Li, J. He, *Corynebacterium humireducens* sp. nov., an alkaliphilic, humic acid-reducing bacterium isolated from a microbial fuel cell, Int. J. Syst. Evol. Microbiol. 61 (2011) 882–887, https://doi.org/10.1099/ijs.0.020909-0.

[55] Q. Liu, B. Liu, W. Li, X. Zhao, W. Zuo, D. Xing, Impact of ferrous iron on microbial community of the biofilm in microbial fuel cells, Front. Microbiol. 8 (2017) 1–9, https://doi.org/10.3389/fmicb.2017.00920.

[56] X. Mei, C. Guo, B. Liu, Y. Tang, D. Xing, Shaping of bacterial community structure in microbial fuel cells by different inocula, RSC Adv. 5 (2015) 78136–78141, https://doi.org/10.1039/c5ra16382j.

[57] S. Ishii, T. Shimoyama, Y. Hotta, K. Watanabe, Characterization of a filamentous biofilm community established in a cellulose-fed microbial fuel cell, BMC Microbiol. 8 (2008) 1–12, https://doi.org/10.1186/1471-2180-8-6.

[58] F. Enzmann, F. Mayer, M. Rother, D. Holtmann, Methanogens: biochemical background and biotechnological applications, AMB Express. 8 (2018) 1–22, https://doi.org/10.1186/s13568-017-0531-x.

[59] J. Kalimuthu, V. Gadhamshetty, B. Vemuri, J. Islam, S. Dhiman, R. Sani, Extracellular electron transfer capabilities of phenotypically improved methylotrophs, SIMB Annu. Meet. Exhib. (2019, 2019:) 36.

[60] S.M. Wilson, M.P. Gleisten, T.J. Donohue, Identification of proteins involved in formaldehyde metabolism by *Rhodobacter sphaeroides*, Microbiology 154 (2008) 296–305, https://doi.org/10.1038/jid.2014.371.

[61] M.T. Wong, D. Cheng, R. Wang, I.M. Hsing, Modifying the endogenous electron fluxes of *Rhodobacter sphaeroides* 2.4.1 for improved electricity generation, Enzyme Microb. Technol. 86 (2016) 45–51, https://doi.org/10.1016/j.enzmictec.2016.01.009.

[62] Y.K. Cho, T.J. Donohue, I. Tejedor, M.A. Anderson, K.D. McMahon, D.R. Noguera, Development of a solar-powered microbial fuel cell, J. Appl. Microbiol. 104 (2008) 640–650, https://doi.org/10.1111/j.1365-2672.2007.03580.x.

[63] Islam J., Chilkoor G., Jawaharraj K., Dhiman S.S., Sani R., Gadhamshetty V., Vitamin-C-enabled reduced graphene oxide chemistry for tuning biofilm phenotypes of methylotrophs on nickel electrodes in microbial fuel cells, Bioresour. Technol. 300 (2020) 1 – 7, https://doi.org/10.1016/j.biortech.2019.122642 122642.

[64] J.H.F.G. Heijthuijsen, T.A. Hansen, Interspecies hydrogen transfer in co-cultures of methanol-utilizing acidogens and sulfate-reducing or methanogenic bacteria, FEMS Microbiol. Lett. 38 (1986) 57–64, https://doi.org/10.1016/0378-1097(86)90042-X.

[65] A.J. Schink, B., & Stams, Syntrophism among prokaryotes. The Prokaryotes, Dworkin M, Springer, New York, 309-335., 2006.
[66] N. Ulrich, V. Kirchner, R. Drucker, J.R. Wright, C.J. McLimans, T.C. Hazen, M.F. Campa, C.J. Grant, R. Lamendella, Response of aquatic bacterial communities to hydraulic fracturing in Northwestern Pennsylvania: A five-year study, Sci. Rep. 8 (2018) 1–12, https://doi.org/10.1038/s41598-018-23679-7.
[67] M. Takeuchi, H. Ozaki, S. Hiraoka, Y. Kamagata, S. Sakata, H. Yoshioka, W. Iwasaki, Possible cross-feeding pathway of facultative methylotroph *Methyloceanibacter caenitepidi* Gela4 on methanotroph *Methylocaldum marinum* S8, PLoS ONE 14 (2019) 1–19, https://doi.org/10.1371/journal.pone.0213535.
[68] A. Puskas, E.P. Greenberg, S. Kaplan, A.L. Schaefer, A quorum-sensing system in the free-living photosynthetic bacterium *Rhodobacter sphaeroides*, J. Bacteriol. 179 (1997) 7530–7537, https://doi.org/10.1128/jb.179.23.7530-7537.1997.
[69] Y.C. Yong, Y.Y. Yu, C.M. Li, J.J. Zhong, H. Song, Bioelectricity enhancement via overexpression of quorum sensing system in *Pseudomonas aeruginosa*-inoculated microbial fuel cells, Biosens. Bioelectron. 30 (2011) 87–92, https://doi.org/10.1016/j.bios.2011.08.032.
[70] D.R. Learman, H. Yi, S.D. Brown, S.L. Martin, G.G. Geesey, A.M. Stevens, M.F. Hochella, Involvement of *Shewanella oneidensis* MR-1 LuxS in biofilm development and sulfur metabolism, Appl. Environ. Microbiol. 75 (2009) 1301–1307, https://doi.org/10.1128/AEM.01393-08.
[71] E.T. Sayed, N.A.M. Barakat, M.A. Abdelkareem, H. Fouad, N. Nakagawa, Yeast extract as an effective and safe mediator for the baker's-yeast-based microbial fuel cell, Ind. Eng. Chem. Res. 54 (2015) 3116–3122, https://doi.org/10.1021/ie5042325.
[72] M. Masuda, S. Freguia, Y.F. Wang, S. Tsujimura, K. Kano, Flavins contained in yeast extract are exploited for anodic electron transfer by *Lactococcus lactis*, Bioelectrochemistry 78 (2010) 173–175, https://doi.org/10.1016/j.bioelechem.2009.08.004.
[73] S. Chen, X. Jing, J. Tang, Y. Fang, S. Zhou, Quorum sensing signals enhance the electrochemical activity and energy recovery of mixed-culture electroactive biofilms, Biosens. Bioelectron. 97 (2017) 369–376, https://doi.org/10.1016/j.bios.2017.06.024.
[74] W. Hwang, K.E. Lee, J.K. Lee, B.C. Park, K.S. Kim, Genes of *Rhodobacter sphaeroides* 2.4.1 regulated by innate quorum-sensing signal, 7,8-cis-N-(tetradecenoyl) homoserine lactone, J. Microbiol. Biotechnol. 18 (2008) 219–227.
[75] Zhang W., Zhang F., Li Y.X., Jiang Y., Zeng R.J., No difference in inhibition among free acids of acetate, propionate and butyrate on hydrogenotrophic methanogen of Methanobacterium formicicum , Bioresour. Technol. 294 (2019) 1 – 7, https://doi.org/10.1016/j.biortech.2019.122237 122237.
[76] B. Zhang, Z. Wang, J. Shi, H. Dong, Sulfur-based mixotrophic bio-reduction for efficient removal of chromium (VI) in groundwater, Geochim. Cosmochim. Acta. 268 (2020) 296–309, https://doi.org/10.1016/j.gca.2019.10.011.
[77] J. Shi, B. Zhang, R. Qiu, C. Lai, Y. Jiang, C. He, J. Guo, Microbial chromate reduction coupled to anaerobic oxidation of elemental sulfur or zerovalent iron, Environ. Sci. Technol. 53 (2019) 3198–3207, https://doi.org/10.1021/acs.est.8b05053.
[78] Y. Gao, J. Lee, J.D. Neufeld, J. Park, B.E. Rittmann, H.S. Lee, Anaerobic oxidation of methane coupled with extracellular electron transfer to electrodes /631/61/168 /631/326/2522 /14/32 article, Sci. Rep. 7 (2017) 1–9, https://doi.org/10.1038/s41598-017-05180-9.
[79] P. Parameswaran, C.I. Torres, H.S. Lee, R. Krajmalnik-Brown, B.E. Rittmann, Syntrophic interactions among anode respiring bacteria (ARB) and non-ARB in a biofilm anode: Electron balances, Biotechnol. Bioeng. 103 (2009) 513–523, https://doi.org/10.1002/bit.22267.
[80] H. Ren, H.S. Lee, J. Chae, Miniaturizing microbial fuel cells for potential portable power sources: Promises and challenges, Microfluid. Nanofluidics. 13 (2012) 353–381, https://doi.org/10.1007/s10404-012-0986-7.
[81] J.N. Roy, H.R. Luckarift, C. Lau, A. Falase, K.E. Garcia, L.K. Ista, P. Chellamuthu, R. P. Ramasamy, V. Gadhamshetty, G. Wanger, Y.A. Gorby, K.H. Nealson, O. Bretschger, G.R. Johnson, P. Atanassov, A study of the flavin response by *Shewanella* cultures in carbon-limited environments, RSC Adv. 2 (2012) 10020–10027, https://doi.org/10.1039/C2RA21727A.